A comparison of popular beamforming arrays

Zebb Prime (1) and Con Doolan (1)

(1) School of Mechanical Engineering, The University of Adelaide, SA, AUSTRALIA

ABSTRACT

Beamforming is a popular method of acoustic source localisation using an array of microphones. When beamforming over a plane or a series of planes, these microphone arrays are often two-dimensional sparse patterns of various designs. The design of these patterns is non-trivial, and influences the achievable resolution, also referred to as the beamwidth, and the Maximum Sidelobe Levels (MSL), a measure of the ability of the array to reject sources that the array is not focussed on. Although recent deconvolution techniques such as DAMAS aim to remove properties of the array from the results of beamforming, in practice the properties of the array will still influence the quality of the results. For this reason, it is important that the array exhibit good resolution and MSL for the intended beamforming application. In this paper, several popular two-dimensional array patterns such as the patented Underbrink and B&K spirals, as well as Doherty spirals and log-spirals are critically compared for both resolution and MSL for a variety of source locations, including both near-field (spherical propagation) and far-field (planar propagation) sources. Each array compared has an aperture of 1m, and uses 63 microphones in a typical arrangement found for each of the types. As array resolution scales linearly with wavelength, the resolution is calculated at a single frequency of 3 kHz, and normalised against wavelength. The MSL levels are calculated at the one-third octave band centre frequencies from 1–31.5 kHz. Results show that the Underbrink design outperforms other array patterns in both resolution and MSL over the majority of frequencies analysed.

INTRODUCTION

Beamforming is a popular technique where an array of receivers is used to identify transmission sources and/or improve signal to noise ratios of the source originating from a certain point. Applications include radio-telescopes (Napier, Thompson, and Ekers 1983); wireless networking (Love, Heath, and Strohmer 2003); and in acoustics, conference room speaker isolation (Fischer and Simmer 1996); and source localisation for aeroacoustic sources (Arcondoulis et al. 2012).

For scanning over a plane, or a series of planes, microphones are usually placed on a two-dimensional plane. If the microphones are regularly spaced, then they must be placed close together to avoid spatial aliasing, resulting in a requirement for potentially thousands of microphones, which has extreme cost requirements. Instead of using regular microphone spacing, irregular microphone spacing can avoid spatial aliasing for a much more modest expense. In fact, if no common grid of inter-microphone spacings (also known as the co-array) can be established, spatial aliasing can be eliminated, however sidelobes that approach the main lobe in amplitude are often considered effective spatial aliasing (Johnson and Dudgeon 1993). For this reason, successful irregular array designs should have unique inter-microphone spacings, which is known as a non-redundant array design.

Designing a successful irregular array pattern is a non-trivial process, and there have been many attempts to improve the array response for a fixed number of microphones. Several of the more popular configurations are presented below in the array types section. As spiral designs naturally exhibit unique inter-microphone spacings, and hence are naturally non-redundant, many of the currently popular beamformer designs in acoustics use spirals as their base structure.

The response of an array is typically evaluated by simulating or creating a point sound source, then looking at the output over a larger scanning plane. The resulting beam pattern will show how well the array is able to locate a source at a given frequency, also known as its resolution or beamwidth, which varies linearly with frequency; and how well the array is able to reject sound sources that are located away from the focus point, which is determined by the next highest lobe in the array response, referred to as the Maximum Sidelobe Level (MSL).

Recently there has been considerable progress in deconvolution techniques, such as DAMAS (Brooks and Humphreys 2006), which aim to remove the characteristics of the array from the resulting beamformed pattern. Although many of these deconvolution techniques perform well, in practice the properties of the array still influence the results, hence it is important that the array still performs well.

This paper performs a comparison of several popular beamforming array designs, by comparing their beamwidth and MSL over a range of source locations. First, the array types are discussed below in the Array types section, where an effort is made to present equations of each array, as these are often not published. Following this, the methodology for evaluating the array response is introduced, before results and concluding remarks are presented.

ARRAY TYPES

The array types used in this comparison have been taken from several popular designs. Often, the equations to generate the microphone locations have not been published, so a point is made to display all array microphone locations in this work.

Archimedean spiral

The Archimedean spiral array is an array with microphones placed according to the Archimedean spiral equation:

$$r(\theta) = a + b\theta. \tag{1}$$

To design an Archimedean spiral array, the maximum and minimum radii, $r_{\max}$ and r_0 respectively; the number of turns the spiral should turn through, ϕ in radians; and the number of microphones, N, should be selected. The array microphone positions are then:

$$\theta_n = \frac{(n-1)\phi}{N-1}, \quad n = 1,\ldots,N, \text{ and} \tag{2}$$

$$r_n = r_0 + \frac{r_{\max} - r_0}{\phi}\theta_n, \quad n = 1,\ldots,N. \tag{3}$$

The design of an Archimedean spiral is shown in Figure 1.

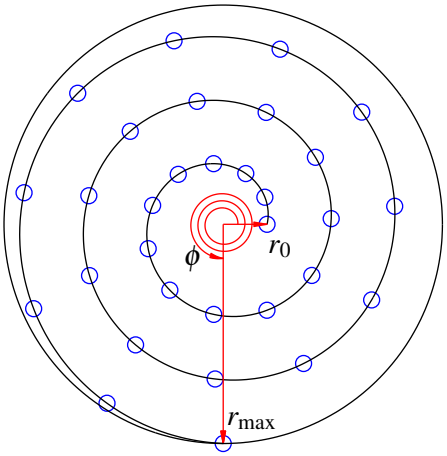

Figure 1. Archimedean spiral array design with $N = 31$, $\phi = 11\pi/2$ rad, and $r_0/r_{\max} = 0.2$.

Dougherty log-spiral

The Dougherty array (Dougherty 1998; Underbrink 2002) is constructed from a logarithmic spiral, with microphones placed at equally spaced arc lengths. The Doherty log-spiral array is designed by choosing the maximum spiral radius, $r_{\max}$, the minimum spiral radius, r_0, the spiral angle, ν (the constant angle at which radii from the origin of the spiral are cut by the spiral curve), and the number of microphones, N. The microphone are then equally spaced along the spiral(Underbrink 2002):

$$l_n = \left(\frac{n-1}{N-1}\right) l_{\max}, \quad n = 1,\ldots,N \tag{4}$$

where:

$$l_{\max} = \frac{r_0\sqrt{1+\cot^2(\nu)}}{\cot(\nu)}\left(\frac{r_{\max}}{r_0} - 1\right). \tag{5}$$

The polar coordinates of the microphones can then be calculated using:

$$\theta_n = \frac{1}{\cot(\nu)} \ln\left(1 + \frac{\cot(\nu) l_n}{r_0\sqrt{1+\cot^2(\nu)}}\right), \quad n = 1,\ldots,N, \text{ and} \tag{6}$$

$$r_n = r_0 e^{\cot(\nu)\theta_n}, \quad n = 1,\ldots,N. \tag{7}$$

The design of the Dougherty log-spiral is illustrated in Figure 2.

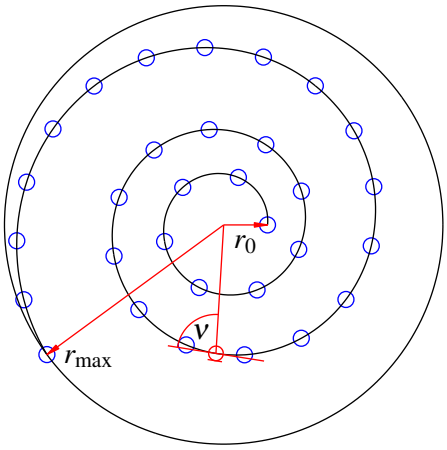

Figure 2. Dougherty log-spiral design with $N = 31$, $\nu = 15\pi/32$ rad, and $r_0/r_{\max} = 0.2$.

Arcondoulis spiral

The Arcondoulis spiral (Arcondoulis et al. 2010) is an exponential spiral modified to place more microphones near the centre, and hence improve the MSL level at high frequencies. The Arcoundoulis spiral is calculated by choosing coefficients a, which affects the overall size of the array, b, which affects how rapidly the spiral extends from the centre, ϕ, the total angle the spiral sweeps through, ε_x and ε_y, parameters which affect the 'squashing' of the spiral in x and y respectively. The microphone locations are then:

$$x_n = \left(\frac{n+\varepsilon_x N}{N}\right) a\cos(\theta_n)\exp(b\theta_n), \quad n = 1,\ldots,N, \text{ and} \tag{8}$$

$$y_n = \left(\frac{n+\varepsilon_y N}{N}\right) a\sin(\theta_n)\exp(b\theta_n), \quad n = 1,\ldots,N, \tag{9}$$

$$\tag{10}$$

where:

$$\theta_n = \left(\frac{(n-1)\phi}{N-1}\right), \quad n = 1,\ldots,N. \tag{11}$$

To simplify the design, if a desired starting radius, r_0, and maximum radius, $r_{\max}$, are known, the coefficients a and b can be calculated to be:

$$a = r_0\left(\frac{N}{\varepsilon_x N + 1}\right) \tag{12}$$

$$b = \frac{1}{\phi}\ln\left(\frac{r_{\max}}{a\sqrt{(1+\varepsilon_x)^2\cos^2\phi + (1+\varepsilon_y)^2\sin^2\phi}}\right) \tag{13}$$

An illustration of the Arcondoulis spiral design is shown in Figure 3.

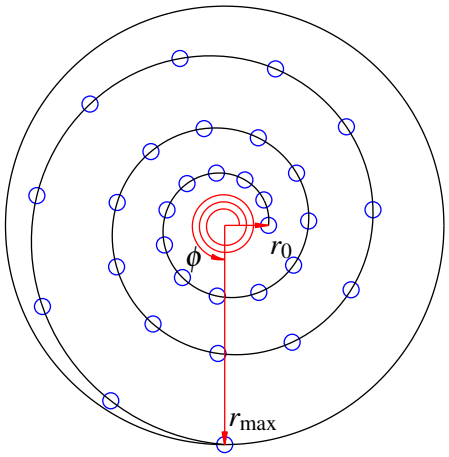

Figure 3. Arcondoulis spiral design with $N = 31$, $\phi = 11\pi/2$ rad, $\varepsilon_x = \varepsilon_y = 0.9$, and $r_0/r_{\max} = 0.2$.

Multi-spiral

The multi-spiral design is based upon using a number of spirals, equally rotated about the origin (Underbrink 2002). The particular spiral to base each arm on can vary; however in this case the log spiral is used.

The procedure for determining microphone positions is to select the maximum and minimum radii, $r_{\max}$ and r_0, the number of spiral arms, N_a, and the number of microphones per spiral N_m, and the spiral angle, ν, then repeat the Dougherty log-spiral

procedure for $N = N_m$ to get $r_{1,n}$ and $\theta_{1,n}$. The spiral arm is then repeated N_a times and equally rotated about the origin:

$$r_{m,n} = r_{1,n}, \quad n = 1,\ldots,N_m, \quad m = 1,\ldots,N_a, \text{ and} \tag{14}$$

$$\theta_{m,n} = \theta_{1,n} + \frac{m-1}{N_a}2\pi, \quad m = 1,\ldots,N_a, \quad n = 1,\ldots,N_m. \tag{15}$$

Finally, if desired, a single microphone is placed in the centre of the array.

An illustration of the multi-spiral design is shown in Figure 4.

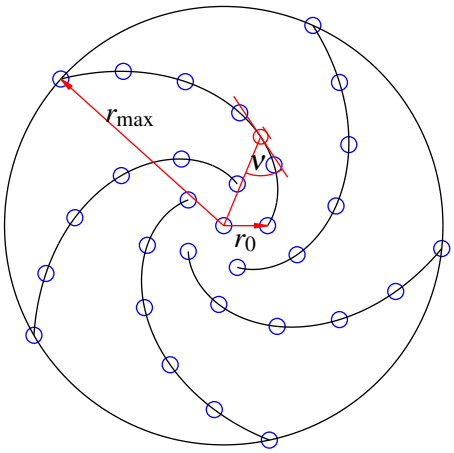

Figure 4. Multi-spiral array design with $N = 31$, $N_a = 5$, $N_m = 6$, $\nu = 5\pi/16$ rad, and $r_0/r_{\max} = 0.2$.

Underbrink array

The Underbrink design (Underbrink 2001; Underbrink 2002) is a modified multi-spiral design, where the microphones are placed in the centre of equal area segments. The procedure for calculating the microphone locations is to select the maximum and minimum (microphone) radii, $r_{\max}$ and r_0, the number of spiral arms, N_a, the number of microphones per spiral N_m, and the spiral angle, ν. The area of the array is then separated into $N_m - 1$ equal area annuli, which are further subdivided into equal area segments, with microphones placed at the centre of these segments. Finally, an inner circle of microphones is added at r_0 to improve the high frequency MSL, and if desired an extra microphone can be placed at the origin. The radii of the microphones are:

$$r_{m,1} = r_0, \quad m = 1,\ldots,N_a \tag{16}$$

$$r_{m,n} = \sqrt{\frac{2n-3}{2N_r-3}}\, r_{\max}, \quad m = 1,\ldots,N_a, \quad n = 2,\ldots,N_m. \tag{17}$$

With the radii of the microphones known, the angles are calculated by placing each microphone along a log spiral, and rotating the spiral around the origin so that there are N_a spiral arms. Thus the angles of the microphones are:

$$\theta_{m,n} = \frac{\ln\left(\frac{r_{m,n}}{r_0}\right)}{\cot(\nu)} + \frac{m-1}{N_a}2\pi, \quad m = 1,\ldots,N_a, \quad n = 1,\ldots,N_m. \tag{18}$$

An illustration of the Underbrink array design is shown in Figure 5.

Brüel & Kjær style array

The Brüel & Kjær (B&K) style array (Christensen and Hald 2006) is designed to be easily assembled and disassembled for

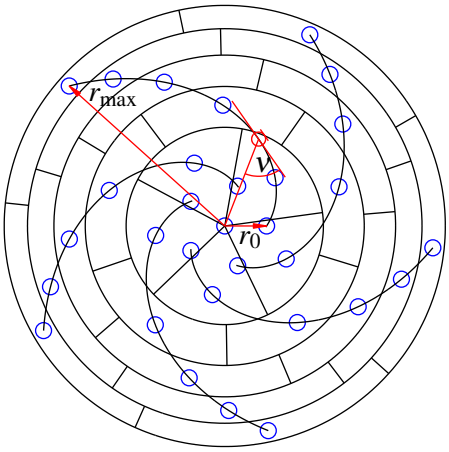

Figure 5. Underbrink array design with $N = 31$, $N_a = 5$, $N_m = 6$, $\nu = 5\pi/16$ rad, $r_0/r_{\max} = 0.2$.

field use, and hence is based around two concentric hoops with microphones located on spokes between the hoops. The spokes themselves are placed at an angle ϕ to the inner hoop (such that $\phi = 90°$ would place the spoke tangential to the inner hoop, and $\phi = 180°$ would place the spoke radially outward), and the microphones have a non-uniform spacing along the spoke. To calculate the microphone locations, the number of spokes, N_a, microphones per spoke, N_m, spoke angle, ϕ, and a distribution of microphone locations along the spoke:

$$d_n \in [0\ 1], \quad n = 1,...,N_m, \tag{19}$$

need to be chosen. The microphone radii can then be calculated as:

$$r_{m,n} = \sqrt{r_0^2 + (ld_n)^2 - 2r_0 ld_n \cos(\phi)}, \quad m = 1,...,N_a, \quad n = 1,...,N_m, \tag{20}$$

where:

$$l = r_0\cos(\phi) + \sqrt{r_{\max}^2 - r_0^2\sin^2(\phi)}. \tag{21}$$

The angles of the microphones are then:

$$\theta_{m,n} = \sin^{-1}\left(\frac{ld_n}{r_{m,n}}\sin(\phi)\right) + \frac{m-1}{N_a}2\pi, \quad m = 1,\ldots,N_a, \quad n = 1,\ldots,N_m. \tag{22}$$

An illustration of the B&K array design is shown in Figure 6.

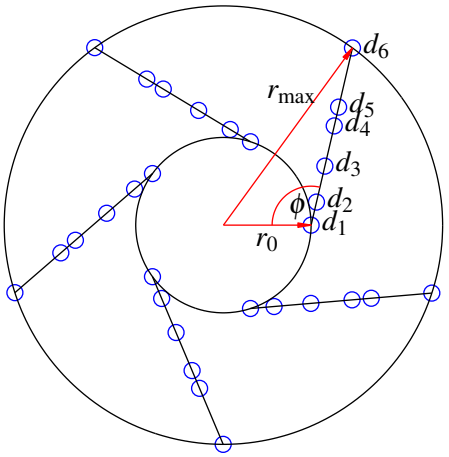

Figure 6. B&K array design with $N = 30$, $N_a = 5$, $N_r = 6$, $r_0/r_{\max} = 0.4$, $\phi = 1.8$ rad, and $d = [0\ 0.13\ 0.333\ 0.56\ 0.666\ 1]$.

Comparison methodology

The different array types were compared for beamwidth and MSL for both near-field (spherical propagation) and far-field (planar propagation), and compared over a range of frequencies. The two comparison methods are explained in more detail below.

Far-field comparison

The equation for the response of a beamformer for a unit pressure planar wave is (Underbrink 2002):

$$W(\vec{k},\vec{k}_0,\vec{x}) = \sum_{n=1}^{N} \frac{e^{j(\vec{k}-\vec{k}_0)\cdot\vec{x}_n}}{N}, \tag{23}$$

where: W is the array response, $\vec{k}$ is the wavenumber vector to focus on, $\vec{k}_0$ is the wavenumber vector of the source, $\vec{x}$ is the vector of microphone locations, and N is the number of microphones.

Due to the direct subtraction of the wavenumber source from the wavenumber focus point in Equation (23), the array response does not change shape with source direction in this wavenumber domain (note that the wavenumber domain does not scale linearly with angle). Hence to compare the arrays, each array's response was evaluated with a source located at $k_{x_0}/k = 0$ and $k_{y_0}/k = 0$, where k_{x_0} and k_{y_0} are the x and y components of the source wavenumber vector, and k is the wavenumber magnitude. The array response was evaluated over a grid of $k_x/k = [-\frac{1}{\sqrt{2}}\ \frac{1}{\sqrt{2}}]$ and $k_y/k = [-\frac{1}{\sqrt{2}}\ \frac{1}{\sqrt{2}}]$ each with 201 equally spaced points, where k_x and k_y are the x and y components of the focus wavenumber.

The response of the array is then converted to decibels:

$$Y(\vec{k},\vec{k}_0,\vec{x}) = 10\log\left(\left|W(\vec{k},\vec{k}_0,\vec{x})\right|^2\right) \tag{24}$$

and the beamwidth was found by searching in 4 directions from the source origin for the -3 dB point, as shown by the 4 arrows in Figure 7, then taking the largest value, k_p/k, converting to an angle, and normalising by the wavelength:

$$BW_p = \frac{2}{\lambda}\sin^{-1}\left(\frac{k_p}{k}\right). \tag{25}$$

The MSL level is determined by excluding the main lobe, which is determined by searching in radial directions from the source origin for the first stationary point (i.e. where $dY/dr = 0$, with r being the radial coordinate), then finding the maximum level outside of this main lobe, as shown in Figure 7.

As the beamwidth scales linearly with wavelength, the beamwidth for each array is only calculated at a single frequency of $f = 3$ kHz. The MSL levels on the other hand tend to increase with frequency, although no simple relationship is evident, and as such they are calculated at a range of frequencies. In this case, the frequencies to calculate the MSL levels are the centre frequencies of the one-third octave bands from $f = 1$ kHz to $f = 31.5$ kHz.

Near-field comparison

When a beamforming array is used with a near-field source, such that the pressure waves propagate spherically, the evaluation of the array performance is less general, and must be performed at the expected array operating conditions.

Instead of scanning over incoming wavenumbers, as per far-field beamforming, near-field beamforming instead scans over a region of space, usually a plane parallel to the plane of the array.

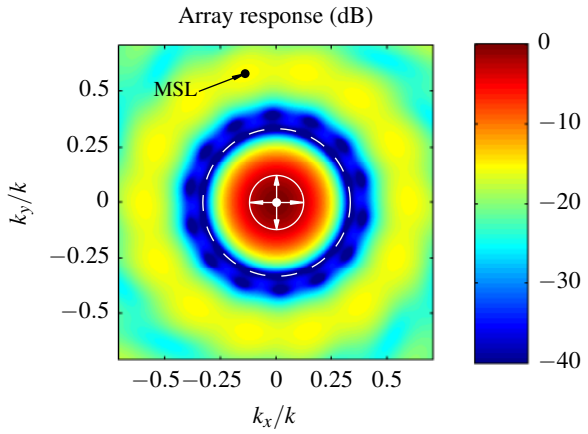

Figure 7. Illustration of the far-field array comparison method. This plot is the response of an Underbrink array with $N = 63$, $N_a = 7$, $N_m = 9$, $r_{\max} = 0.5$ m, $r_0 = 0.02$ m, and $\nu = 3\pi/8$ rad for planar propagation at $f = 1.5$ kHz. The arrows indicate the search directions for determining the main lobe width, and the dashed line indicates the first stationary points from the main lobe, and hence the MSL is the maximum value outside this region.

For this comparison, cartesian coordinates were used, with both the microphone and scanning planes being x–y planes, with $z = 0$ m for the microphone plane, and $z = 0.5$ m for the scanning plane. Specifically, the coordinates of the scanning plane were a regular grid with points:

$$x \in [-0.5\ 0.5]\,\text{m},\ \text{with}\ \Delta x = 0.01\,\text{m} \tag{26}$$
$$y \in [-0.5\ 0.5]\,\text{m},\ \text{with}\ \Delta y = 0.01\,\text{m} \tag{27}$$
$$z = 0.5\,\text{m}. \tag{28}$$

The response of the arrays were analysed using an analytic expression from Underbrink (2002):

$$W(\omega,\vec{x}_p,\vec{x}_s) = \sum_{n=1}^{N} \frac{r_s}{r_n}\exp\left\{j\omega\left[\frac{(r_s - r_p) - (r_n - r'_n)}{c}\right]\right\}, \tag{29}$$

where: W is the array response; ω is the analysis frequency; $\vec{x}_p$ is the focus point; $\vec{x}_s$ is the source location; N is the number of microphones; r_s is the distance from the source to the origin of the array; r_p is the distance from the origin to the focus point; r_n is the distance from the source to the n-th microphone; r'_n is the distance from the n-th microphone to the focus point; and c is the speed of sound (assumed to be 343.21 m/s for this comparison).

As the beamformer response will vary significantly with source location (as opposed to the far-field response), the array responses are evaluated over a grid of source locations:

$$x_s \in [-0.5\ 0.5]\,\text{m},\ \text{with}\ \Delta x = 0.01\,\text{m} \tag{30}$$
$$y_s \in [-0.5\ 0.5]\,\text{m},\ \text{with}\ \Delta y = 0.01\,\text{m} \tag{31}$$
$$z_s = 0.5\,\text{m}. \tag{32}$$

For each source location, the array response was normalised

and converted to decibels:

$$Y(\omega,\vec{x}_p,\vec{x}_s) = 10\log\left(\frac{|W(\omega,\vec{x}_p,\vec{x}_s)|^2}{|W(\omega,\vec{x}_s,\vec{x}_s)|^2}\right), \qquad (33)$$

then the beamwidth was calculated by searching in the tangental and radial directions for the -3 dB point. The maximum value is then used as the beamwidth and normalised against wavelength:

$$BW_{0.5} = \frac{2}{\lambda} l_{\max}, \qquad (34)$$

where the subscript to BW indicates the z depth, and $l_{\max}$ is the maximum length from the search directions. As with the far-field approach, the beamwidth for a near-field source scales linearly with wavelength, hence the beamwidths are only evaluated at a single frequency of $f = 3$ kHz.

The MSL levels were calculated by searching in radial directions from the source for the first stationary point, then finding the maximum value outside of this region. The MSL levels were evaluated over the grid of source locations above, and for the same one-third octave band centre frequencies as used in the Far-field Comparison section. An illustration of this process is shown in Figure 8.

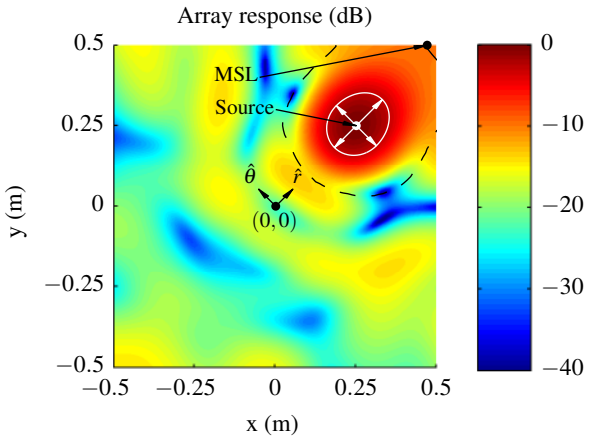

Figure 8. Illustration of the near-field source array comparison method. This plot is the response of an Underbrink array with $N = 63$, $N_a = 7$, $N_m = 9$, $r_{\max} = 0.5$ m, $r_0 = 0.02$ m, and $\nu = 3\pi/8$ rad for spherical propagation at $f = 1.5$ kHz with the source located at $\vec{x} = [0.25\ 0.25\ 0.5]$ m. The arrows indicate the radial and tangential search directions for determining the main lobe width, and the dashed line indicates the first stationary points from the main lobe, and hence MSL is the maximum value outside this region.

Array Parameters

The arrays used in this comparison each used $N = 63$ microphones, and had an aperture of 1 m (hence $r_{\max} = 0.5$ m). The specific parameters for the different array types used in the comparison are given in Table 1. It is worth noting that the parameters used in this comparison have not been optimised. In some instances, such as for the B&K array, the original authors state they have optimised the design, but fail to publish the resulting parameters or microphone locations.

RESULTS

The results and discussion of the array comparison results for both the near-field and far-field sources are given below.

Table 1. Array parameters used in the array comparison. * denotes derived values.

(a) Archimedean spiral

N	63
ϕ	8π rad
r_0	0.005 m
$r_{\max}$	0.5 m

(b) Doherty log-spiral

N	63
ν	$\frac{31}{64}\pi$ rad
r_0	0.01 m
$r_{\max}$	0.5 m

(c) Arcondoulis spiral

N	63
r_0	0.02 m
$r_{\max}$	0.5 m
ϕ	12π rad
ε_x, ε_y	0.9
a^*	0.0218
b^*	0.0660

(d) Multi-spiral

N	63
N_a	7
N_m	9
r_0	0.05 m
$r_{\max}$	0.5 m
ν	$\frac{3}{8}\pi$ rad

(e) Underbrink array

N	63
N_a	7
N_m	9
r_0	0.05 m
$r_{\max}$	0.5 m
ν	$\frac{3}{8}\pi$ rad

(f) B&K style array

N	63
N_a	7
N_m	9
r_0	0.2 m
$r_{\max}$	0.5 m
ϕ	$\frac{\pi}{2}$ rad
$\vec{d}$	[0 0.09 0.233 … 0.333 0.555 0.628 … 0.688 0.895 1]

Far-field comparison results

The far-field results for array resolution are given in Table 2, and the MSL levels versus frequency are shown in Figure 9. The results show that the Underbrink and B&K achieve significantly better array resolutions than the other array types, with the single spiral designs (Doherty, Archimedean and Arcondoulis) performing the worst. The MSL results show that the Multi-spiral, Underbrink and Arcondoulis arrays achieve the lowest MSLs at low, medium and high frequencies respectively, with the B&K and Archimedean design performing poorly.

Table 2. Results of the far-field array comparison resolutions (beamwidths).

Underbrink	1.064 deg/m
B&K	1.083 deg/m
Multi-spiral	1.192 deg/m
Doherty	1.294 deg/m
Archimedean	1.299 deg/m
Arcondoulis	2.003 deg/m

It appears that for the far-field comparison, the Underbrink design provides the best array resolution with good MSLs.

Near-field comparison results

The beamwidth levels for different source locations are shown in Figure 10. The results show that similar to the far-field results, the Underbrink and B&K designs achieve the best array resolutions, and maintain good resolutions for much of the scan plane. Interestingly, the designs based on a single spiral (Archimedean, Doherty and Arcondoulis) exhibit significant distortion in the resolution over the scan plane, which is due to the spiral naturally placing less microphones at the outer radii then multi armed designs.

The MSLs for the arrays with the source located at the centre of the scanning plane is shown in Figure 11, and the MSLs

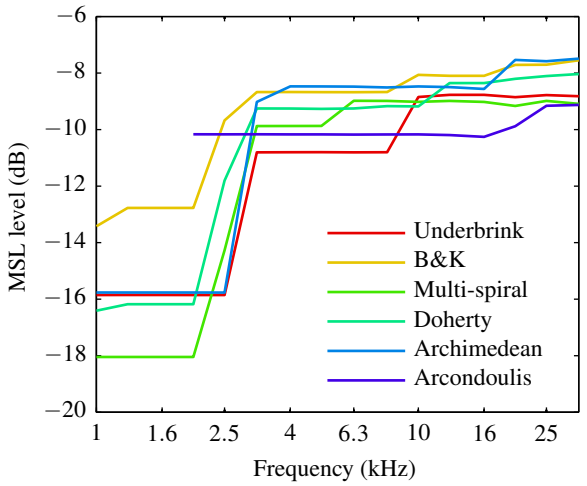

Figure 9. Results of the far-field array comparison MSLs.

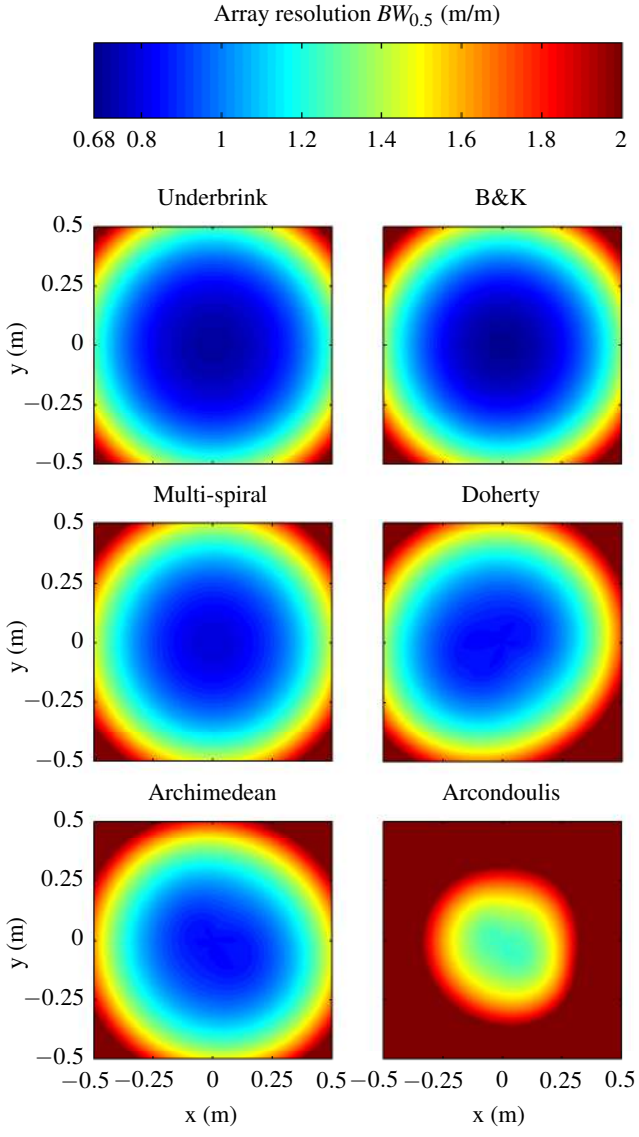

Figure 10. Near-field array resolution (beamwidth) for different source locations.

for the worst-case source location for each array is shown in Figure 12. The results show that the MSL levels for all of the

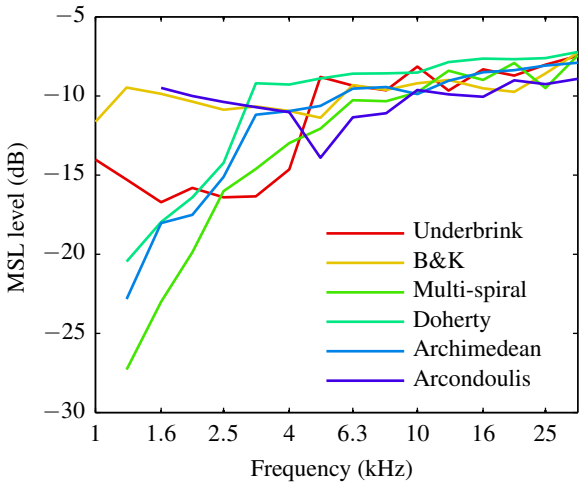

Figure 11. Near-field MSL levels when $\vec{x}_s = [0\ 0\ 0.5]$.

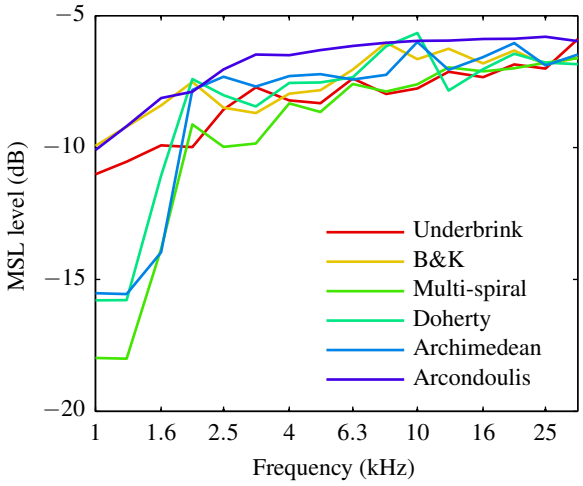

Figure 12. Near-field worst case source location MSL levels.

arrays appears to approach a value of approximately −6 dB as frequencies increase, which is a higher value than from the far-field comparison. When the source is located at the origin, the Arcondoulis spiral appears to have the lowest MSLs above $f = 4$ kHz, closely followed by the B&K, multi-spiral and Underbrink designs. However at frequencies below 2.5 kHz, the Arcondoulis and B&K designs perform poorly.

When considering the worst-case source location MSL, the Arcondoulis spiral performs poorly, with the other single spiral designs (Doherty and Archimedean) performing slightly better. On the other hand, the Underbrink and Multi-spiral designs have the lowest worst-case source location MSLs above $f = 4$ kHz.

This discrepancy between MSL levels for the source at the centre versus worst case is likely due to the distribution of microphones over the array. For the single spiral designs there tend to be a higher density of microphones around the centre of the array, in particular the Arcondoulis spiral which was modified to place more microphones around the centre. This results in better MSLs when the source is located at the origin, at the expense of array resolution and performance when the source is not located directly in front of the centre of the array. In contrast to this, the multi-armed design tend to have a better distribution of microphones around the outer regions of the array, hence providing higher array resolution, and good MSLs

over a larger area, at the expense of higher MSLs directly below the centre of the array.

CONCLUSIONS

Several popular array designs used in acoustic beamforming have been compared for far-field, and near-field applications. The array designs that are based around multiple arms, with microphones more evenly distributed around the array area, tended to achieve the best array resolution with adequate MSLs for most of the area. Array designs with a high density of microphones located at the centre of the array tended to achieve the best MSLs directly below the array, at the expense of array resolution and performance over a larger array area.

Based on the results for both the far-field and near-field source comparisons, the Underbrink style array appears to offer the best all-around performance, with the best array resolution, competitive MSLs when the source is located at the centre, and good MSLs when the source is not located directly below the array.

REFERENCES

Arcondoulis, Elias J. G., Con J. Doolan, Anthony C. Zander, and Laura A. Brooks (2010). "Design and Calibration of a Small Aeroacoustic Beamformer". *Proceedings of the 20th International Congress on Acoustics*. Sydney, Australia, 23–27 August. DOI: 10.1109/CAR.2010.5456775.

Arcondoulis, Elias J. G., Con J. Doolan, Laura A. Brooks, and Anthony C. Zander (2012). "On the generation of airfoil tonal noise at zero angle of attack and low to moderate Reynolds number". *18th AIAA/CEAS Aeroacoustics Conference*. Colorado Springs, CO, USA, 04–06 June. DOI: 10.2514/6.2012-2060.

Brooks, Thomas F. and William M. Humphreys (2006). "A deconvolution approach for the mapping of acoustic sources (DAMAS) determined from phased microphone arrays". *Journal of Sound and Vibration* 295.4–5, pp. 856–879. DOI: 10.1016/j.jsv.2005.12.046.

Christensen, Jacob Juhl and Jorgen Hald (2006). "Beam forming array of transducers". Pat. US 7,098,865 B2.

Dougherty, Robert P. (1998). "Spiral-shaped array for broadband imaging". Pat. US 5,838,284.

Fischer, Sven and Klaus Uwe Simmer (1996). "Beamforming microphone arrays for speech acquisition in noisy environments". *Speech Communication* 20.3–4, pp. 215–227. DOI: 10.1016/S0167-6393(96)00054-4.

Johnson, Don H. and Dan E. Dudgeon (1993). *Array Signal Processing: Concepts and Techniques*. Upper Saddle River, NJ, USA: Prentice Hall.

Love, David J., Robert W. Jr. Heath, and Thomas Strohmer (2003). "Grassmannian beamforming for multiple-input multiple-output wireless systems". *IEEE Transactions on Information Theory* 49.10, pp. 2735–2747. DOI: 10.1109/TIT.2003.817466.

Napier, Peter J., A. Richard Thompson, and Ronald D. Ekers (1983). "The Very Large Array: Design and performance of a modern synthesis radio telescope". *Proceedings of the IEEE* 71.11, pp. 1295–1320. DOI: 10.1109/PROC.1983.12765.

Underbrink, J. R. (2001). "Circularly symmetric, zero redundancy, planar array having broad frequency range applications". Pat. US 6,205,224 B1.

Underbrink, James R. (2002). "Aeroacoustic Phased Array Testing in Low Speed Wind Tunnels". *Aeroacoustic Measurements*. Ed. by Thomas J. Mueller. Berlin: Springer. Chap. 3, pp. 98–217. ISBN: 3-540-41757-5.